AIP | Applied Physics Letters

AlInAsSb/GaSb staircase avalanche photodiode

Min Ren, Scott Maddox, Yaojia Chen, Madison Woodson, Joe C. Campbell, and Seth Bank

Citation: Applied Physics Letters **108**, 081101 (2016); doi: 10.1063/1.4942370
View online: http://dx.doi.org/10.1063/1.4942370
View Table of Contents: http://scitation.aip.org/content/aip/journal/apl/108/8?ver=pdfcov
Published by the AIP Publishing

AlInAsSb/GaSb staircase avalanche photodiode

Min Ren,[1,a)] Scott Maddox,[2,a)] Yaojia Chen,[1] Madison Woodson,[1] Joe C. Campbell,[1] and Seth Bank[2]
[1]*Department of Electrical and Computer Engineering, University of Virginia, Charlottesville, Virginia 22904, USA*
[2]*Microelectronics Research Center, University of Texas, Austin, Texas 78758, USA*

(Received 9 January 2016; accepted 5 February 2016; published online 22 February 2016)

Over 30 years ago, Capasso and co-workers [IEEE Trans. Electron Devices **30**, 381 (1982)] proposed the staircase avalanche photodetector (APD) as a solid-state analog of the photomultiplier tube. In this structure, electron multiplication occurs deterministically at steps in the conduction band profile, which function as the dynodes of a photomultiplier tube, leading to low excess multiplication noise. Unlike traditional APDs, the origin of staircase gain is band engineering rather than large applied electric fields. Unfortunately, the materials available at the time, principally $Al_xGa_{1-x}As$/GaAs, did not offer sufficiently large conduction band offsets and energy separations between the direct and indirect valleys to realize the full potential of the staircase gain mechanism. Here, we report a true staircase APD operation using alloys of a rather underexplored material, $Al_xIn_{1-x}As_ySb_{1-y}$, lattice-matched to GaSb. Single step "staircase" devices exhibited a constant gain of ~2×, over a broad range of applied bias, operating temperature, and excitation wavelengths/intensities, consistent with Monte Carlo calculations. © *2016 AIP Publishing LLC*.
[http://dx.doi.org/10.1063/1.4942370]

Optical communications and sensing often require higher sensitivity than a p-i-n photodiode can provide.[1–3] In many cases, improved performance can be achieved with avalanche photodiodes (APDs). However, the gain in an APD originates from impact ionization, a stochastic process marked by gain variations. These gain fluctuations are a source of noise that is characterized by a figure of merit referred to as the excess noise factor, *F(M)*.[4–6] High excess noise factors degrade sensitivity and limit the gain-bandwidth product. Much of the research on new materials and structures for APDs has been directed at reducing the excess noise factor. One approach has been to identify materials with advantageous impact ionization characteristics such as Si,[7–10] $Hg_{0.7}Cd_{0.3}Te$,[11,12] or InAs.[13–17] Another approach to achieving low noise is by incorporating new materials and impact ionization engineering with appropriately designed heterostructures.[18] One particularly compelling structure, the staircase APD, was proposed by Capasso and co-workers[19] to achieve very low noise.[6] Conceptual band diagrams of a staircase APD at flatband and under reverse bias are illustrated in Fig. 1. Unlike conventional APDs, in which impact ionization occurs relatively uniformly throughout the entire multiplication region, in the staircase structure impact ionization events occur proximate to sharp bandgap discontinuities, which function similarly to dynodes in a photomultiplier tube. Unfortunately, initial studies of staircase APDs focused on the $Al_xGa_{1-x}As$ material system, which has inadequate band offsets to achieve the projected avalanche gain characteristics.[20,21]

In this paper, we report a staircase APD based on the emerging $Al_xIn_{1-x}As_ySb_{1-y}$ material system (subsequently referred to as AlInAsSb), which is grown by molecular beam epitaxy (MBE) using a digital alloying technique.[22,23] The wide bandgap injector is $Al_{0.7}In_{0.3}As_{0.31}Sb_{0.69}$ and the narrow bandgap multiplication region is $InAs_{0.91}Sb_{0.09}$ (InAsSb in the following). These regions have bandgaps of ~1.16 eV and ~0.25 eV, respectively, as determined by photoluminescence measurements.[23] Since the conduction band discontinuity (~0.6 eV) provides over twice the energy of the narrow bandgap InAsSb layer (~0.25 eV),[23] and the threshold for impact ionization in small-bandgap III-V's is approximately 1.5× the bandgap,[24] this is sufficient to provide a high probability of impact ionization at the bandgap discontinuity. The AlInAsSb material system provides the additional benefit of a low ratio of hole to electron ionization coefficients, or *k*-value, further suppressing excess noise.[25,26] To demonstrate the AlInAsSb staircase gain mechanism, 1-step staircase APD and control structures were grown on n^+ GaSb substrates; the structure cross-sections are shown in

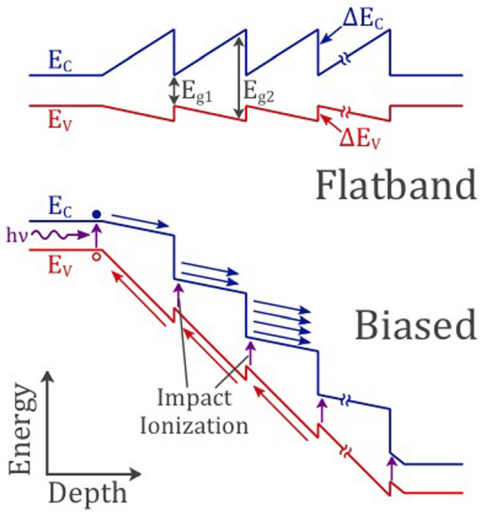

FIG. 1. Conceptual band diagrams of a staircase APD unbiased (top) and under reverse bias (bottom). The arrows below the valance band indicate that holes do not impact ionize.

[a)]M. Ren and S. Maddox contributed equally to this work.

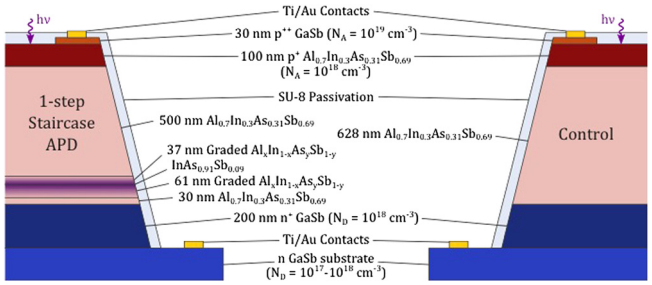

FIG. 2. Schematic cross-sections of the 1-step AlInAsSb staircase APD (left) and control (right) structures that were investigated.

Fig. 2. The control device facilitated determination of the unity gain photocurrent, which was employed to establish the gain in the 1-step staircase APD. Figure 3 shows the band structure of the 1-step AlInAsSb staircase APD and step-free control that was used to determine the unity gain point. The staircase "step" was formed by digitally grading from $Al_{0.7}In_{0.3}As_{0.31}Sb_{0.69}$ to $InAs_{0.91}Sb_{0.09}$, then back to $Al_{0.7}In_{0.3}As_{0.31}Sb_{0.69}$. The grading rates on either side of the InAsSb were chosen such that, at sufficiently high bias, the band edges in the graded layers "flatten" to form the staircase-condition band structure shown in Fig. 3. Note that the graded layers serve to reduce charge trapping and accumulation within the small-bandgap region.

The device structures were grown on n-type GaSb (001) substrates at a growth temperature of 480 °C, as determined by blackbody thermometry (k-Space BandiT). Solid-source valved crackers provided As_2 and Sb fluxes, and solid-source effusion cells provided Al, Ga, In, Be (acceptor), and GaTe (donor) fluxes. The AlInAsSb layers were grown as digital alloys of stable binaries using a repeating shutter sequence: AlSb, AlAs, AlSb, InSb, InAs, and Sb. Layer thicknesses, alloy fractions, and doping concentrations were confirmed by secondary ion mass spectrometry. Further growth details and optical properties of the resulting material are reported elsewhere.[23] Circular mesas were defined with standard photolithograph process and chemically etched with $HCl:H_2O_2:H_2O$ (1:1:5). The top p^+ GaSb layer was removed by AZ 400 developer[18] in the center of the mesa to form a window

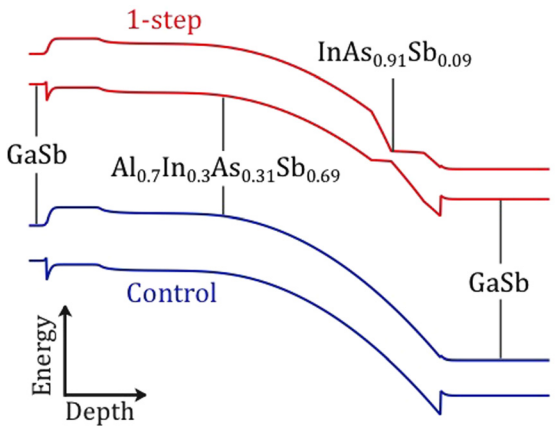

FIG. 3. Band diagrams of the 1-step (top) and control (bottom) structures at the staircase condition.

region. Immediately following the mesa etch, the exposed sidewalls were passivated with SU-8, common photoresist that has been found to provide low surface leakage. Titanium/gold contacts were deposited by e-beam evaporation on the top of mesa and on the substrate.

In order to develop a deeper understanding of the electron and hole transport and impact ionization dynamics in these structures, we performed detailed Monte Carlo simulations using the tool reported in Ref. 27. The results are summarized in Fig. 4. Notably, these simulations predicted electron-only impact ionization, as shown in Fig. 4(a), with a spatial distribution highly localized at the small-bandgap staircase step. Furthermore, the simulations predict an extremely sharp gain distribution independent of bias as shown in Fig. 4(b) with almost all electrons (>95%) impact ionizing exactly once, resulting in a nearly excess-noise-free gain of ~2×. This level of determinism results in an excess noise factor very close to unity.[6,19] The predicted variance, $\langle M^2\rangle - \langle M\rangle^2$, of the multiplication gain, M, was less than 0.05 for reverse biases less than 4 V. Essentially, the Monte Carlo simulations predict that the AlInAsSb staircase gain would be almost completely free of excess noise, making it possible to achieve much greater performance and bandwidth than traditional APDs.

Initial experiments focused on devices with $Al_{0.7}In_{0.3}As_{0.31}Sb_{0.69}$ absorption regions, which exhibit a cutoff wavelength of ~1.1 μm, in order to simplify analysis by bypassing charge-injection issues. The temperature dependence of the dark current was measured in a liquid-nitrogen-cooled, low-temperature chamber. The dark current versus mesa-diode area at 2 V and 3 V reverse bias is plotted in Fig. 5(a). The decrease in dark current with diameter is quadratic, indicating that bulk generation-recombination dominated surface leakage. As shown in Fig. 5(b), for a 50 μm-diameter device the dark current is in the low picoamp range at low temperature and bias. For bias less than 2 V, the primary source of dark current is generation-recombination. At higher bias, tunneling becomes the dominant mechanism. For gain measurements, a 543 nm He-Ne CW laser was used as the optical source, in order to ensure pure electron injection into the multiplication region. The multiplication gain of the staircase APDs was determined by comparing their photocurrent to that of the control devices. To eliminate device-to-device variations, 40 devices of each type (i.e., staircase and control) were measured, and results were replicated over multiple growth and fabrication runs. Figure 6 shows representative photocurrent curves as a function of the bias voltage for the 1-step staircase and control photodiodes under the same optical input power. The multiplication gain was found to be 1.8 ± 0.2 independent of reverse bias in the range from 1 V to 4 V. The multiplication gain remains constant in the temperature range from 80 K to 300 K. This is consistent both with the theory for staircase gain[6,28,29] and with the Monte Carlo simulations. Beyond 4 V reverse bias, the 1-step photocurrent increases. This may be due to carriers gaining additional kinetic energy from the wide bandgap field and impact ionizing in the narrow bandgap AlInAsSb layer and GaSb layer as they would in a conventional APD. The increased gain, when biased beyond 4 V, has also been observed in Monte Carlo simulation. Wafers without composition grading between the

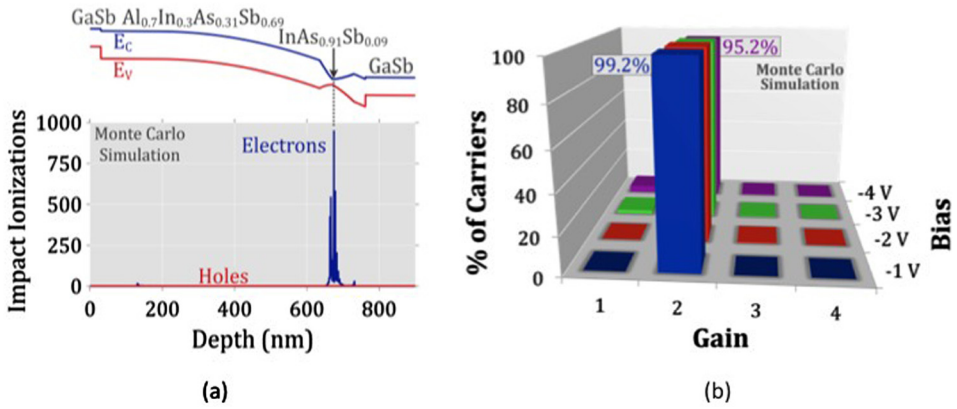

FIG. 4. Monte Carlo simulations of a 1-step AlInAsSb staircase APD at −2 V bias (a) predict electron-only impact ionization, resulting in nearly ideal noise characteristics. Furthermore, the simulations predict an extremely sharp gain distribution independent of bias (b) with almost all electrons impact ionizing exactly once, resulting in a nearly excess-noise-free gain of ∼2×.

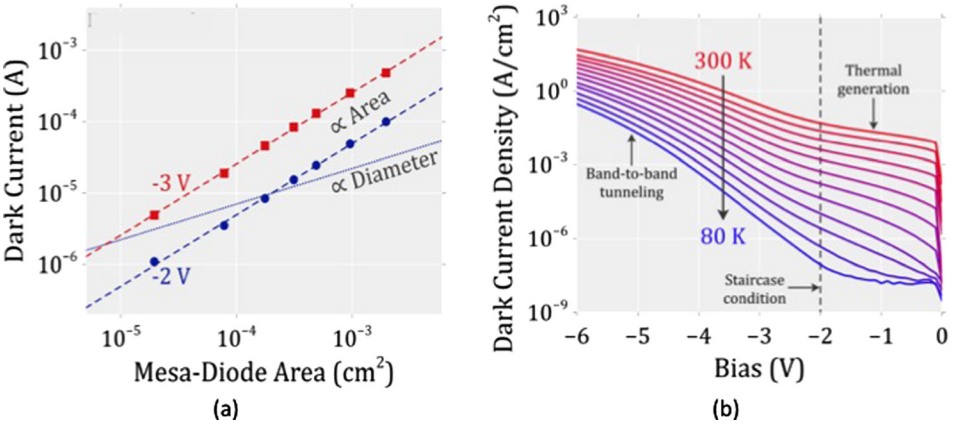

FIG. 5. The 1-step staircase APD exhibited bulk-dominated dark currents for all mesa-diode diameters ranging from 50 μm to 500 μm (a), and the dark current densities at the staircase condition ranged from moderate at room temperature to very low at liquid-nitrogen temperatures (b). The temperature dependence was consistent with thermal generation at low reverse biases and band-to-band tunneling at high reverse biases.

AlInAsSb injection region and the InAsSb layer exhibited gain values of 1.6 ± 0.2 for bias in the range 1 V to 4 V. The different gain between staircase APDs with and without composition grading is possibly due to the higher scattering rate of the $Al_{0.7}In_{0.3}As_{0.31}Sb_{0.69}$/InAsSb heterojunction interface, which dissipates some of the electron kinetic energy. In order to verify that the increased photocurrent in the 1-step staircase was not due to enhanced absorption in the small-bandgap step, we performed spectral responsivity measurements. The resulting spectra for the 1-step staircase and control devices are shown in Fig. 7. As expected, for wavelengths longer than ∼950 nm, the 1-step staircase exhibited greater responsivity than the control, due to absorption in the small-bandgap step. More importantly, however, we observed an approximately constant 1-step gain of 1.8 ± 0.2 over a broad range of wavelengths shorter than ∼950 nm, ruling out enhanced absorption and confirming impact ionization as the source of the observed gain. Note that the small shaking of spectral data in Figure 7 is due to the resonant effect of SU-8 coating.

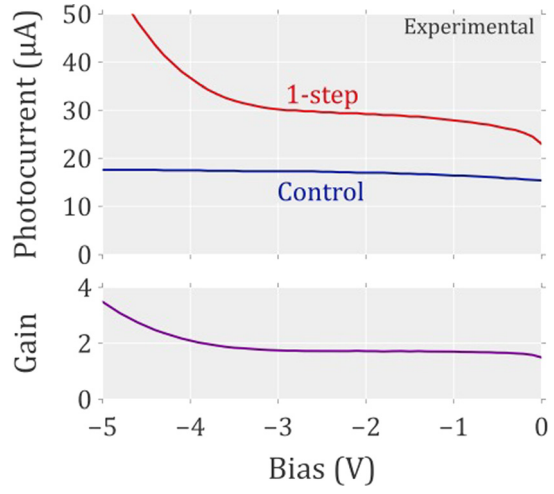

FIG. 6. The 1-step staircase APD exhibited enhanced photocurrent compared to the control at all reverse biases and a gain of 1.8 ± 0.2 from −1 V to −4 V. The measurement was performed on a 50 μm diameter mesa device at room temperature using a CW He-Ne laser operating at 543 nm He-Ne wavelength.

In order to confirm the low-noise characteristics of the multiplication gain, the noise power spectra density was measured as a function of bias The noise power spectral density, φ, is related to the excess noise factor, $F(M)$, by the equation $\varphi = 2qIF(M)R(\omega)$, where q is the charge of the electron, I is the primary photo current, M is the mean value of multiplication gain, and $R(\omega)$ is the device impedance.[4,5] Since the noise power scales as the square of the gain, the noise of the staircase device is expected to be 3.2× and 2.6× that of the control photodiode for the structures with and without compositional grading between the AlInAsSb and InAsSb layers. The measured noise was only 2 to 2.2 times that of the control device. While fortuitous, this unexpectedly low noise will be the subject of future study. It should be noted that Ma *et al.*, have previously observed similar noise suppression in impact-ionization engineered (I^2E) heterojunction APDs.[30]

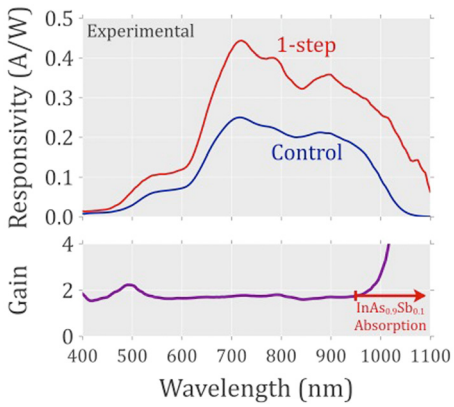

FIG. 7. The 1-step staircase APD exhibited a gain of 1.8 ± 0.2 over a broad range of wavelengths shorter than ~950 nm, ruling out enhanced absorption and confirming impact ionization as the source of the observed gain. All data were measured at room temperature (300 K).

In this paper, we have demonstrated a low-noise 1-step staircase APD based on the AlInAsSb material system. By taking advantage of the large ratio of the conduction-band discontinuity to the threshold energy between $Al_{0.7}In_{0.3}As_{0.31}Sb_{0.69}$ and $InAs_{0.91}Sb_{0.09}$, we have demonstrated a near-ideal gain of 1.8 ± 0.2 per step, resulting in highly deterministic and low-noise operation. By utilizing the wide range of effective bandgaps available from AlInAsSb digital alloys and both InAs/GaSb and InAs/InAsSb type-II strained-layer superlattices (SLSs), it will additionally be possible to develop separate absorption, charge, and multiplication (SACM) AlInAsSb staircase APDs with cutoff wavelengths ranging throughout the short-wave and mid-wave infrared bands. The near-ideal gain characteristics combined with the availability of large-format GaSb wafers and the relatively high yield of III-V compound semiconductor devices make AlInAsSb staircase APDs a promising platform on which to build enhanced night vision, thermal imaging, and free-space telecommunications capabilities. We note that higher gain can be achieved by incorporating more steps in the multiplication region. This will be the subject of future work.

This work has been supported by the Army Research Office and DARPA under Contract No. W911NF-10-1-0391.

[1]R. G. Smith and S. D. Personick, "Receiver design for optical fiber communications systems," in *Semiconductor Devices for Optical Communication* (Springer-Verlag, New York, 1980), Chap. 4.
[2]S. R. Forrest, "Sensitivity of avalanche photodetector receivers for high-bit-rate long-wavelength optical communication systems," in *Semiconductors and Semimetals: Lightwave Communications Technology* (Academic Press, 1985), Vol. 22, Chap. 4.
[3]B. L. Kasper and J. C. Campbell, J. Lightwave Technol. **5**, 1351 (1987).
[4]R. J. McIntyre, IEEE Trans. Electron Devices **13**, 164 (1966).
[5]N. Z. Hakim, B. E. A. Saleh, and M. Teich, IEEE Trans. Electron Devices **37**, 599 (1990).
[6]M. Teich, K. Matsuo, and B. E. A. Saleh, IEEE J. Quantum Electron. **22**, 1184 (1986).
[7]C. A. Lee, R. A. Logan, R. L. Batdorf, J. J. Kleimack, and W. Weigmann, Phys. Rev. **134**, A761J (1964).
[8]J. Conradi, IEEE Trans. Electron Devices **19**, 713 (1972).
[9]W. N. Grant, Solid-State Electron. **16**, 1189 (1973).
[10]T. Kaneda, H. Matsumoto, and T. Yamaoka, J. Appl. Phys. **47**, 3135 (1976).
[11]J. D. Beck, C. F. Wan, M. A. Kinch, and J. E. Robinson, Proc. SPIE **4454**, 188 (2001).
[12]J. D. Beck, C.-F. Wan, M. A. Kinch, J. E. Robinson, F. Ma, and J. C. Campbell, in *2003 IEEE LEOS Annual Meeting Conference Proceedings* (2003), Vol. 2, p. 849.
[13]A. R. J. Marshall, C. H. Tan, M. J. Steer, and J. P. R. David, Appl. Phys. Lett. **93**, 111107 (2008).
[14]A. R. J. Marshall, P. J. Ker, A. Krysa, J. P. R. David, and C. H. Tan, Opt. Express **19**, 23341 (2011).
[15]W. Sun, S. J. Maddox, S. R. Bank, and J. C. Campbell, in *72nd Annual Device Research Conference, Santa Barbara, CA, 2014*, p. 47.
[16]W. Sun, Z. Lu, X. Zheng, J. C. Campbell, S. J. Maddox, H. P. Nair, and S. R. Bank, IEEE J. Quantum Electron. **49**, 154 (2013).
[17]P. J. Ker, A. R. J. Marshall, A. B. Krysa, J. P. R. David, and C. H. Tan, in *2012 Opto-Electronics and Communications Conference (OECC), Busan, South Korea, 2012*, p. 220.
[18]J. C. Campbell, S. Demiguel, F. Ma, A. Beck, X. Guo, S. Wang, X. Zheng, X. Li, J. D. Beck, M. A. Kinch, A. Huntington, L. A. Coldren, J. Decobert, and N. Tscherptner, IEEE J. Sel. Top. Quantum Electron. **10**, 777 (2004).
[19]F. Capasso, IEEE Trans. Nucl. Sci. **30**, 424 (1983).
[20]G. Ripamonti, F. Capasso, A. L. Hutchinson, D. J. Muehlner, J. F. Walker, and R. J. Malik, Nucl. Instrum. Methods Phys. Res., Sect. A **288**, 99 (1990).
[21]M. Toivonen, A. Salokatve, M. Hovinen, and M. Pessa, Electron. Lett. **28**, 32 (1992).
[22]L. G. Vaughn, L. R. Dawson, H. Xu, Y. Jiang, and L. F. Lester, in *Characterization of AlInAsSb and AlGaInAsSb MBE-grown Digital Alloys*, edited by C. C. Jagadish, M. O. Manasreh, B. D. Weaver, and S. Zollner (Mater. Res. Soc. Symp. Proc., 2003), Vol. 744, p. M7.2.1.
[23]S. J. Maddox and S. R. Bank, "Broadly Tunable AlInAsSb Digital Alloys Grown on GaSb," J. Cryst. Growth Des. (submitted).
[24]J. Bude and K. Hess, J. Appl. Phys. **72**, 3554 (1992).
[25]J. Xie, S. Xie, R. C. Tozer, and C. H. Tan, IEEE Trans. Electron Devices **59**, 1475 (2012).
[26]R. D. Baertsch, J. Appl. Phys. **38**, 4267 (1967).
[27]F. Ma, X. Li, J. C. Campbell, J. D. Beck, C.-F. Wan, and M. A. Kinch, Appl. Phys. Lett. **83**, 785 (2003).
[28]F. Capasso, W.-T. Tsang, and G. F. Williams, IEEE Trans. Electron Devices **30**, 381 (1982).
[29]K. Matsuo, M. C. Teich, and B. E. A. Saleh, J. Lightwave Technol. **3**, 1223 (1985).
[30]F. Ma, S. Wang, and J. C. Campbell, Phys. Rev. Lett. **95**, 176604 (2005).